Materials Today Communications 35 (2023) 105775

Contents lists available at ScienceDirect

Materials Today Communications

journal homepage: www.elsevier.com/locate/mtcomm

Research on performance of smart concrete materials and self-monitoring of cracks in beam members

Jiuyang Li [a,1], Li Chen [a,*], Guangchao Hu [a], Jinpeng Guo [a], Zhenwei Wang [a], Wenbo Lu [a], Jingwei Luo [a], Xinmei Fan [a], Yuepeng Zhu [a], Xiaoyu Wang [a,2], Wenzhong Zhu [a,b]

[a] School of Civil Engineering, Changchun Institute of Technology, Changchun 130012, China
[b] School of Comp, Eng & Physical Sciences, University of the West of Scotland, Scotland, PA12BE, UK

ARTICLE INFO

Keywords:
Smart concrete
Fracture self-monitoring
Bending toughness
Electrical conductivity
Mechanical properties

ABSTRACT

Due to adverse factors such as load and environment exposure, concrete structures often work with cracks during their service period. The occurrence and growth of cracks significantly reduces safety and durability of the structures. It is thus significant to track and monitor cracks in concrete structures in real-time. This paper studies strength, toughness, and crack self-monitoring performance of a large number of smart concrete mixes through addition of two conductive materials, i.e., steel fiber and nano carbon black, into the concrete. Firstly, effect of adding the individual and hybrid conductive materials to concrete mixes on compressive strength, bending toughness and electrical conductivity was investigated. This was followed by studying crack self-monitoring performance and mechanism of the smart concrete beam members under load. The research provides insight and new results of material properties and crack self-monitoring performance in research and development of low-cost smart concrete.

1. Introduction

Buildings often suffer from damages and deteriorations during service due to various loads and environmental factors, including earthquakes, which negatively affect their safety and service life. Therefore, structural health monitoring has always been a research hotspot of many researchers [1]. Structural health monitoring (SHM) refers to collecting and processing information on the location and extent of structural damage and other relevant factors through sensors in normal use stage of a building, to provide a basis for assessing structural safety and service life [2–4]. It plays a crucial role in evaluating the safety and durability of structures. One of the most challenging problems in structural health monitoring is diagnosing and monitoring cracks in structures [5].

At present, the technologies for monitoring concrete cracks include methods based on impact echo [6], ultrasonic [7], acoustic emission [8], ground detection radar [9], optical fiber [10], GPS monitoring [11], etc. Different methods can be used to determine the presence, location, width, and depth of cracks, which greatly improves the efficiency and accuracy of detection [12]. Nevertheless, these technologies face several challenges, such as insufficient durability of optical fiber sensors [13], the inability of acoustic emission technology to detect stable concrete defects [14,15], interference from factors such as lack of GPS signals [16], etc. Such problems objectively limit the application of current technology in practical engineering.

In recent years, smart concrete materials have been researched by many experts and scholars. By ensuring mechanical properties of concrete while enhancing its electrical conductivity to enable crack self-monitoring performance, integration of stress/strain and health monitoring in concrete structures could be achieved. Enrique[17,18] et al. adopted carbon nanotubes as the main material of strain sensors in concrete. Liugenjin [19] studied the influence of different combinations of nanocarbon black, steel fiber, and carbon fiber and their dosage on the sensitivity coefficient of crack self-monitoring. Monteiro et al. [20] studied the effect of adding nano-carbon black on the toughness of concrete. Heng Zhen [21] reported the influence of steel fiber and nanocarbon black on the agility of concrete beams during bending cracking. Chung et al. [22] used carbon black nanoparticles to partially replace carbon fiber and conducted an experimental study on the

* Corresponding author.
E-mail address: 1063915947@qq.com (L. Chen).
[1] ORCID: 0000-0002-7813-8451
[2] ORCID: 0000-0003-1179-1912

https://doi.org/10.1016/j.mtcomm.2023.105775
Received 29 December 2022; Received in revised form 4 March 2023; Accepted 7 March 2023
Available online 11 March 2023

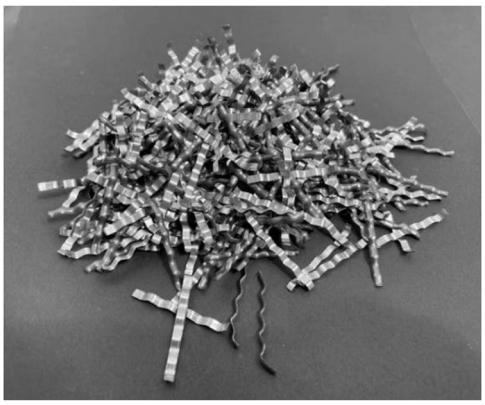

Fig. 1. Milled steel fiber.

Table 1
Main technical specifications of steel fiber.

Length (mm)	Diameter (mm)	Length to diameter ratio	Tensile strength (MPa)	Density(g/cm^3)
38	2.1	18.1	600-1000	7.85

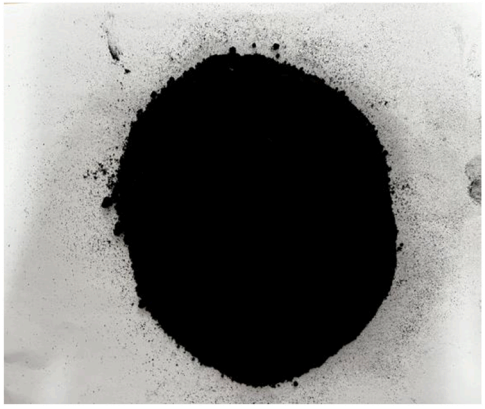

Fig. 2. Nano carbon black.

Table 2
Performance parameters of nano carbon black.

Average particle size (nm)	Density(g/cm^3)	Resistivity(Ω·cm)	Nitrogen adsorption specific surface area (m^2/g)	Iodine absorption value (mg/g)
21	0.4	0.65 ~ 0.85	720	1000

Table 3
Concrete mix design (unit : kg/m3) .

Water cement ratio	Sand ratio	Water	Cement	Sand	Stone	Water Reducer/ (%)
0.62	41	184	307	804	1155	2.3025

pressure sensitivity of cement-based composites.

Based on the previous research, this study investigates smart concrete mixes with addition of two conductive materials, i.e., steel fiber and nano carbon black. Firstly, concrete mixes with addition of different dosages of the individual and hybrid conductive materials were tested to

Table 4
Content of conductive phase material.

Type of conducting phase	Specimen number	Steel fiber	Nano carbon black
Control group	PC	0	0
Single phase	SF-05	39 kg/m^3	0
	SF-10	78 kg/m^3	0
	SF-15	117 kg/m^3	0
	SF-20	156 kg/m^3	0
	NC-25	0	0.76 kg/m^3
	NC-50	0	1.52 kg/m^3
	NC-75	0	2.28 kg/m^3
	NC-100	0	3.04 kg/m^3
Complex phase	SF-05-NC-25	39 kg/m^3	0.76 kg/m^3
	SF-10-NC-25	78 kg/m^3	0.76 kg/m^3
	SF-15-NC-25	117 kg/m^3	0.76 kg/m^3
	SF-20-NC-25	156 kg/m^3	0.76 kg/m^3
	SF-05-NC-50	39 kg/m^3	1.52 kg/m^3
	SF-10-NC-50	78 kg/m^3	1.52 kg/m^3
	SF-15-NC-50	117 kg/m^3	1.52 kg/m^3
	SF-20-NC-50	156 kg/m^3	1.52 kg/m^3
	SF-05-NC-75	39 kg/m^3	2.28 kg/m^3
	SF-10-NC-75	78 kg/m^3	2.28 kg/m^3
	SF-15-NC-75	117 kg/m^3	2.28 kg/m^3
	SF-20-NC-75	156 kg/m^3	2.28 kg/m^3
	SF-05-NC-100	39 kg/m^3	3.04 kg/m^3
	SF-10-NC-100	78 kg/m^3	3.04 kg/m^3
	SF-15-NC-100	117 kg/m^3	3.04 kg/m^3
	SF-20-NC-100	156 kg/m^3	3.04 kg/m^3

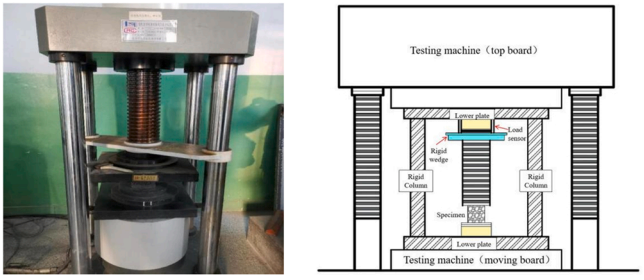

Fig. 3. Compressive strength testing machine.

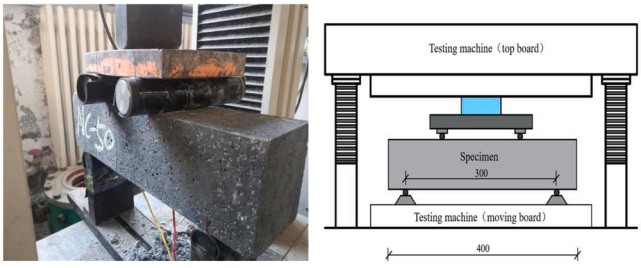

Fig. 4. Bending toughness test device.

determine the optimal dosage of hybrid conductive materials in smart concrete for achieving suitable compressive strength, bending toughness, and electrical conductivity. This was followed by studying crack self-monitoring performance of the smart concrete beam members under load. By exploring the relationship among load, crack, deflection, and

Table 5
Compressive strength test results of intelligent coagulation.

Specimen number	Compressive strength (MPa)	Specimen number	Compressive strength (MPa)	Specimen number	Compressive strength MPa)
PC	31.53	SF-05-NC-25	32.55	SF-05-NC-75	33.54
SF-05	32.54	SF-10-NC-25	34.72	SF-10-NC-75	33.58
SF-10	34.69	SF-15-NC-25	35.66	SF-15-NC-75	34.66
SF-15	35.65	SF-20-NC-25	36.18	SF-20-NC-75	37.77
SF-20	36.73	SF-05-NC-50	31.65	SF-05-NC-100	32.27
NC-25	31.63	SF-10-NC-50	33.43	SF-10-NC-100	33.67
NC-50	31.74	SF-15-NC-50	35.54	SF-15-NC-100	35.54
NC-75	32.33	SF-20-NC-50	36.65	SF-20-NC-100	36.33
NC-100	31.33	–	–	–	–

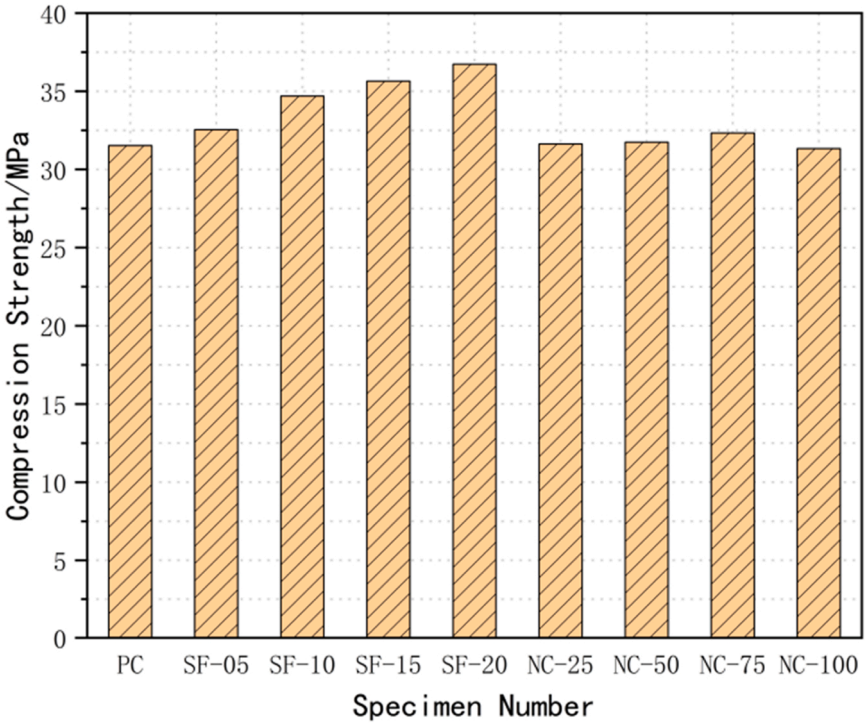

Fig. 5. Compressive strength of smart concrete mixes with individual conductive materials.

resistance change rate, the crack self-monitoring mechanism of intelligent concrete beam members under concentrated load is proposed for the first time, This research provides new insight and results of concrete material properties and crack self-monitoring performance in research and development of low-cost smart concrete.

2. Materials and concrete mix designs

2.1. Materials

The cement used was ordinary Portland cement (P.O 42.5 R). The fine aggregate used was natural river sand with a fineness modulus of 2.41 and particle size of 0–5 mm. The coarse aggregate was ordinary crushed stone with a particle size of 5–10 mm; A powder type naphthalene-based superplasticizer was also used. A milling type steel fibre was selected based on results of initial trials. The fiber was made using steel ingot milling process, with anchored ends and a smooth surface in one side & a rough surface in the other side. The shape of the milling steel fiber is shown in Fig. 1, and its characteristic parameters are presented in Table 1. The wavy curved shape of the fibre leads to an increased contact area between concrete and the fibre, effectively improving the mechanical properties of concrete.,A highly conductive HG-1 P grade nano-carbon black produced by Shandong Tuoxing Chemical Technology Co., LTD was also adopted in this study. The appearance and the performance parameters of the carbon black are shown in Fig. 2 and Table 2, respectively.

2.2. Concrete mixes used

A plain concrete (PC) mix with a C30 strength grade was used as a control. Its mix proportions are shown in Table 3. Based on the control mix, a total of 24 different smart concrete mixes were designed by incorporating various amount of individual conductive materials (i.e. steel fibre (SF) or nano carbon black (NC)) or hybrid conductive materials (i.e. combination of SF and NC). Details of these mixes are presented in Table 4. As shown in Table 4, the steel fiber (SF) content varied from 0.5 %, 1 %, 1.5–2 % of the volume of concrete, and the nano-carbon black (NC) dosages were 0.25 %, 0.5 %, 0.75 % and 1 % of the cement content by weight.

2.3. Specimen preparation and curing

The following procedures were used for specimen preparation and curing:

(1) Apply mould release oil and label the specimen moulds.

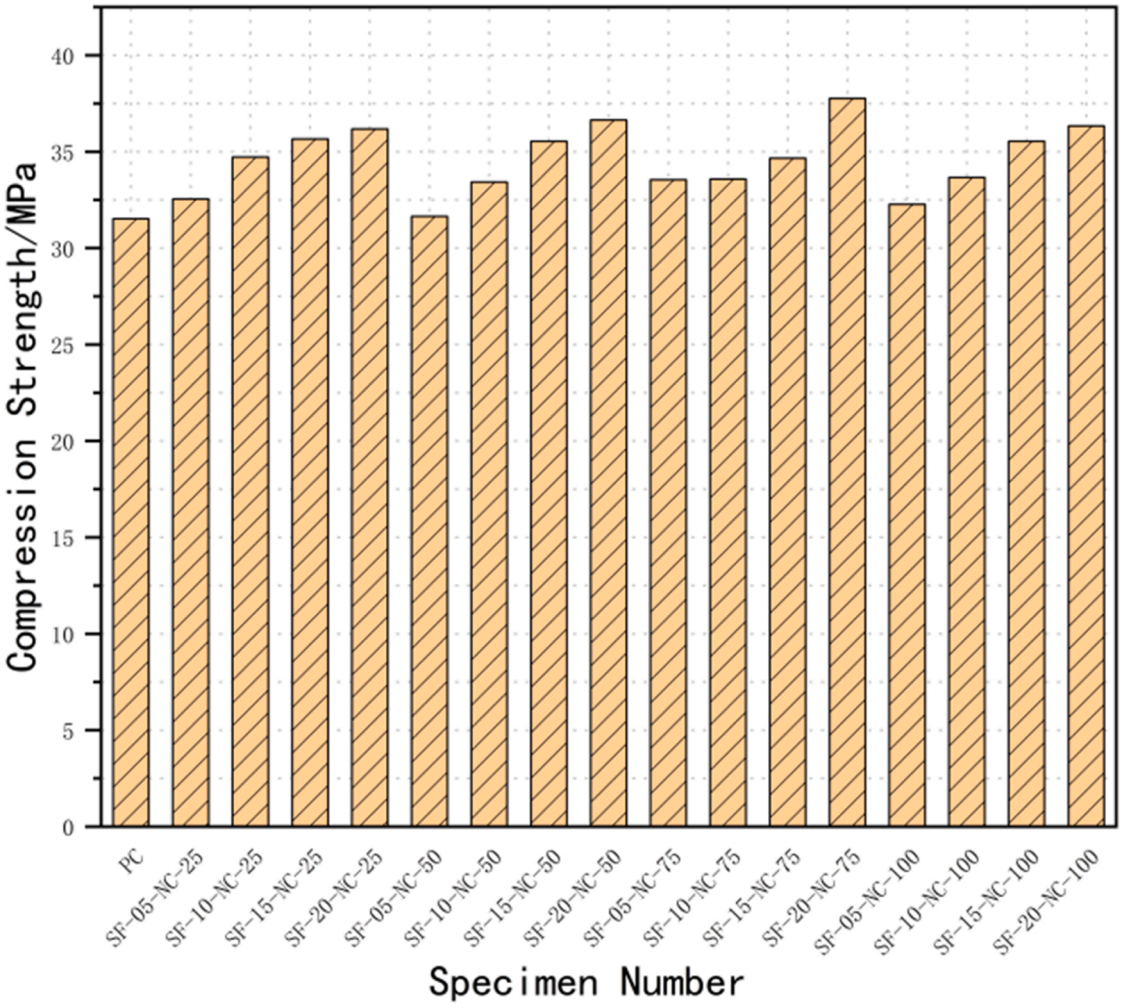

Fig. 6. Compressive strength of smart concrete mixes with hybrid conductive materials.

(2) Mixing cement and the aggregates evenly in a forced-action horizontal single shaft concrete mixer first before adding nano carbon black and continuing mixing for another minute.
(3) Evenly sprinkle steel fibers and mix for 3 min to fully disperse them. The advantage of the dry mixing of steel fiber is that it could achieve more evenly dispersion of steel fibres and reduce the risk of forming fibre balls/clusters in the mixer.
(4) Add batched water to the dry mix, and finally add water reducer. Continue mixing the concrete for another minute.
(5) Place the mixed concrete materials in the prepared molds, and compact them on a vibration table for about 30 s
(6) Demould the concrete specimens the next day and place them in a standard curing room for curing. The curing period is 28 days.

3. Mechanical properties test of smart concrete

3.1. Test method

The addition of steel fiber and carbon black nanoparticles should not negatively impact on the mechanical properties of the concrete matrix, in order to enhance the engineering application value of the prepared smart concrete. Therefore, the smart concrete produced must meet the basic designed mechanical properties.

3.1.1. Compressive strength test

The standard of test method for physical and mechanical properties of concrete (GB/T 50081-2019) [22] was adopted. The size of the concrete specimen was 100 mm × 100 mm × 100 mm, and the 28-day compressive strength of the concrete was determined. The strength of the benchmark concrete, i.e. PC is C30. The compression test was carried out on the 2000 kN microcomputer controlled electro-hydraulic servo hydraulic pressure testing machine (Fig. 3) in the materials Laboratory of Changchun Institute of Technology.

3.1.2. Bending toughness test

ASTM C1609 method [23], with specimen size of 100 mm × 100 mm × 400mmwas used to determine bending toughness of the smart concrete. The load-deflection curve was obtained using the four-point bending method. The test setup is shown in Fig. 4. The net span length is 300 mm, and the pure bending section is 100 mm.

The bending toughness is calculated according to Formula (1):

$$f = \frac{PL}{bd^2} \tag{1}$$

In the formula, f is strength (Pa). P is load (N). b is width of cross section of beam specimen (m) /d is height of cross section (m) of D-beam specimen). L is net span length (m).

In this experiment, five indexes were used to evaluate the bending performance of smart concrete.

(1) The initial peak load P_1 is determined by the experimental curve, and then the initial peak strength f_1 is calculated according to Formula (1).

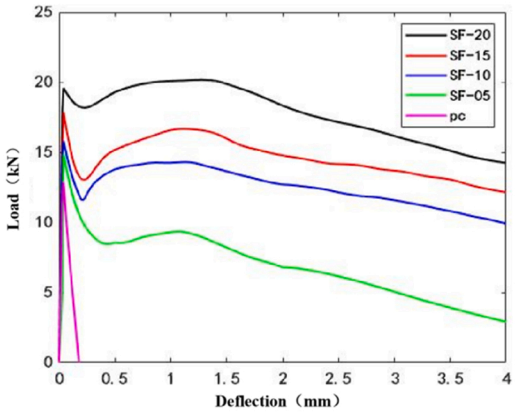

a). single - doped steel fiber

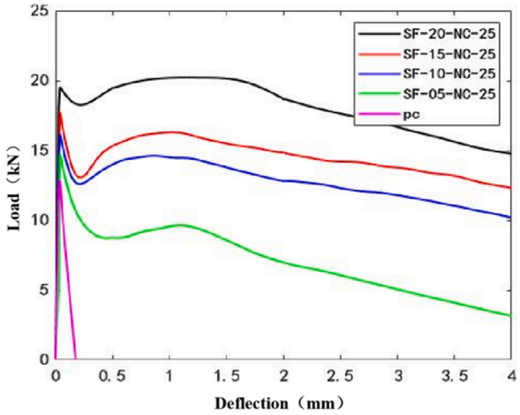

b). steel fiber and carbon black nanoparticles(0.25%)

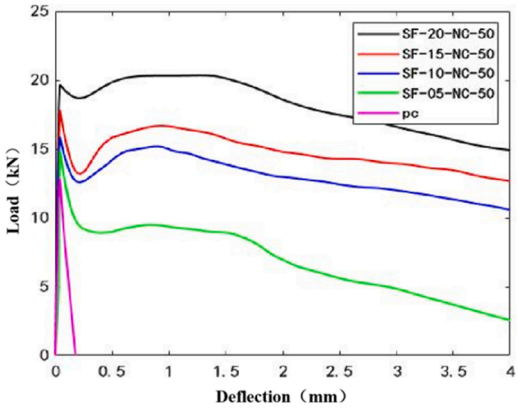

c).steel fiber and carbon black nanoparticles(0.5%)

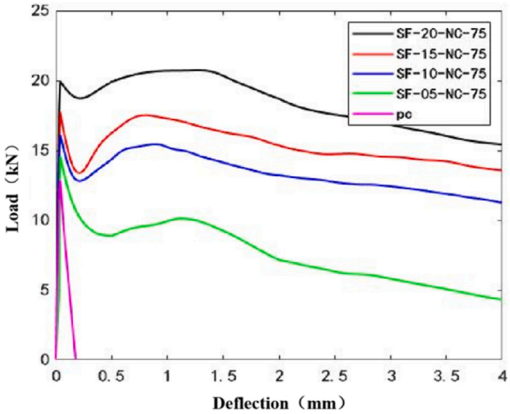

d).steel fiber and carbon black nanoparticles(0.75%)

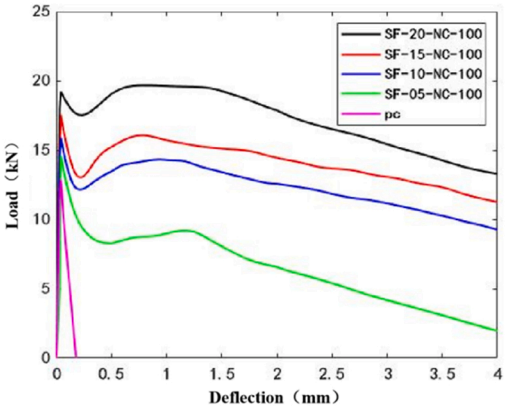

e).steel fiber and carbon black nanoparticles(1%)

Fig. 7. Representative load-deflection curves of the smart concrete beams.

(2) Take the mid-span deflection of L / 600 and L / 150 corresponding to the residual load value P^D_{600} and P^D_{150}, then according to Formula (1) calculate the residual load strength f^D_{600} and f^D_{150}.

(3) T^D_{600} and T^D_{150} are used to express the energy absorption value, and the area enclosed by the load-deflection curve is integrally calculated when the mid-span deflection is L / 600 and L / 150.

(4) The equivalent bending strength ratio $R^D_{T,150}$, the formula is as follows:

$$R^D_{T,150} = \frac{150 \cdot T^D_{150}}{f \cdot b \cdot d^2} \times 100\% \quad (2)$$

It can be obtained from Eqs. (2) and (3).

Table 6
The deflection corresponding to the initial load, flexural strength and peak load of the smart concrete beam.

Specimen number	P_1 (kN)	f_1 (MPa)	δ_1 (mm)
PC	12.88	3.864	0.0244
SF-05	14.87	4.461	0.0257
SF-10	15.79	4.737	0.0311
SF-15	17.89	5.367	0.0341
SF-20	19.58	5.874	0.0376
NC-25	12.98	3.894	0.0288
NC-50	13.22	3.966	0.0321
NC-75	13.56	4.068	0.0345
NC-100	12.69	3.807	0.0387
SF-05-NC-25	14.75	4.425	0.0284
SF-10-NC-25	16.19	4.857	0.0332
SF-15-NC-25	17.76	5.328	0.0356
SF-20-NC-25	19.55	5.865	0.0383
SF-05-NC-50	14.89	4.467	0.0284
SF-10-NC-50	15.89	4.767	0.0332
SF-15-NC-50	17.87	5.361	0.0356
SF-20-NC-50	19.68	5.904	0.0383
SF-05-NC-75	14.56	4.368	0.0277
SF-10-NC-75	16.13	4.839	0.0343
SF-15-NC-75	17.76	5.328	0.0367
SF-20-NC-75	19.75	5.925	0.0397
SF-05-NC-100	14.57	4.371	0.0284
SF-10-NC-100	15.89	4.767	0.0331
SF-15-NC-100	17.55	5.265	0.0363
SF-20-NC-100	19.23	5.769	0.0388

Table 7
smart concrete toughness index.

Specimen number	P^D_{600}kN	f^D_{600} MPa	T^D_{600} N·m	P^D_{150}kN	f^D_{150} MPa	T^D_{150} N·m
SF-05	8.56	2.568	4.674	6.78	2.034	17.026
SF-10	13.78	4.134	6.347	12.69	3.807	26.814
SF-15	15.23	4.569	6.975	14.78	4.434	29.996
SF-20	19.31	5.793	8.845	18.32	5.496	38.554
SF-05-NC-25	8.76	2.628	4.798	6.98	2.094	17.440
SF-10-NC-25	13.98	4.194	6.375	12.79	3.837	27.039
SF-15-NC-25	15.33	4.599	6.991	14.88	4.464	30.827
SF-20-NC-25	19.51	5.853	9.041	18.64	5.592	38.611
SF-05-NC-50	8.98	2.694	4.852	6.98	2.094	17.914
SF-10-NC-50	14.21	4.263	6.549	12.97	3.891	27.541
SF-15-NC-50	15.87	4.761	7.090	14.78	4.434	30.543
SF-20-NC-50	19.87	5.961	9.139	18.56	5.568	39.111
SF-05-NC-75	8.87	2.661	4.867	7.14	2.142	18.109
SF-10-NC-75	14.35	4.305	6.555	13.23	3.969	27.928
SF-15-NC-75	16.23	4.869	7.120	15.38	4.614	31.898
SF-20-NC-75	19.94	5.982	9.262	18.72	5.616	39.538
SF-05-NC-100	8.26	2.478	4.798	6.57	1.971	17.441
SF-10-NC-100	13.45	4.035	6.375	12.57	3.771	27.039
SF-15-NC-100	15.21	4.563	7.000	14.45	4.335	30.827
SF-20-NC-100	19.09	5.727	9.040	17.89	5.367	38.554

$$R^D_{T,150} = \frac{T^D_{150} / \frac{L}{150}}{P_1} \times 100\% \quad (3)$$

3.2. Compressive strength

3.2.1. Compressive strength test results

According to the Standard of Test Methods for Mechanical Properties of Ordinary Concrete (GB/T50081–2019)[22], the arithmetic means value of the measured values of three specimens in each group shall be taken as the strength value of this group. If the difference between the maximum or minimum value and the median value exceeds 15 %, the strength value of this group shall be discarded; if both of them exceed 15 % of the median value, the test will fail. After calculation and analysis, the standard strength values of each concrete mixes with individual and hybrid conductive material additions are presented in Table 5.

3.2.2. Compressive strength of smart concrete with additions of individual conductive materials

The compressive strength results of smart concrete with a additions of individual conductive materials are plotted in Fig. 5.

It could be seen in Table 5 and Fig. 5 that: addition of steel fibre significantly increased compressive strength of the concrete mix, with the 28-day strength increased progressively from 31.53 MPa (with 0 % SF) to 36.79 MPa (with 2 % SF)The main reason for such strength increases could be due to the steel fibers restraining deformation and inhibiting development/spread of microcracks. The good bonding formed between the steel fiber and the matrix and bond slips and pulling out of fibres also contribute to the improvement in compressive strength and higher energy consumed during the test of the smart concrete mixes.

As for the addition of carbon black nanoparticles, its impact on the compressive strength was not as significant, when compared to the cases of steel fibre addition. If anything, only minor strength increases (less than 2.54 %) for concrete mixes with NCB dosage from 0.25 % to 1 % were observed, and possibly with a peak at 0.75 % NCB addition.

3.2.3. Compressive strength of smart concrete mixes with hybrid conductive materials

The compressive strength results of smart concrete mixes with the hybrid conductive materials are plotted in Fig. 6.

Results in Table 5 and Fig. 6 appear to confirm that significant increase in compressive strength could be achieved for smart concrete mixes with addition of hybrid conductive materials. The best combination of the hybrid seemed to be 2 % SF and 0.75 % NCB. It is possible that the addition of nano-carbon black, due to the likely particle packing effect, may contribute to void reduction in concrete further improvement in bond between steel fiber and the matrix.

3.3. Bending toughness

3.3.1. Bending toughness test results

The four-point bending test was carried out and the bending toughness of the smart concrete beam specimens was analyzed as described in Section 3.1.2. After analyzing the load and deflection data collected during the test, the corresponding deflection at the initial load, flexural strength, and the initial peak load of the smart concrete beams were obtained, as shown in Table 8. The representative load-deflection curves of all the smart concrete mixes are presented in five groups in Fig. 7.

Results in Fig. 7 and Table 6 show that the initial peak load and the flexural strength of the smart concrete mixes increases significantly with increase of steel fibre content and a strain-hardening characteristics could be seen when steel fibre content reaches 2 %. It is noted that the area underneath the load-deflection curve, an indicator of toughness, also increases considerably with the steel fibre content. Even a low 0.5 % SF addition in the concrete mix could lead to a ductile failure of the specimens.

Compared to the effect of SF addition, the effect of NCB addition on peak load and flexural strength of the concrete mixes were found to be not as significant, and generally similar to its effect on the compressive strength discussed above. It is interesting to note that the optimal dosage for the nano carbon black appears to be 0.75 % NCB. It is believed that when the optimal amount of carbon black nanoparticles is exceeded, the carbon black nanoparticles could form a continuous film/layer outside the cement particles and thus preventing/reducing further hydration and resulting in the reduction of the initial peak load and flexural strength.

3.3.2. Bending toughness index

3.3.2.1. Residual load P^D_{600}、P^D_{150} *and residual strength* f^D_{600}、f^D_{150}. Table 7 summaries the residual load and the energy absorption values

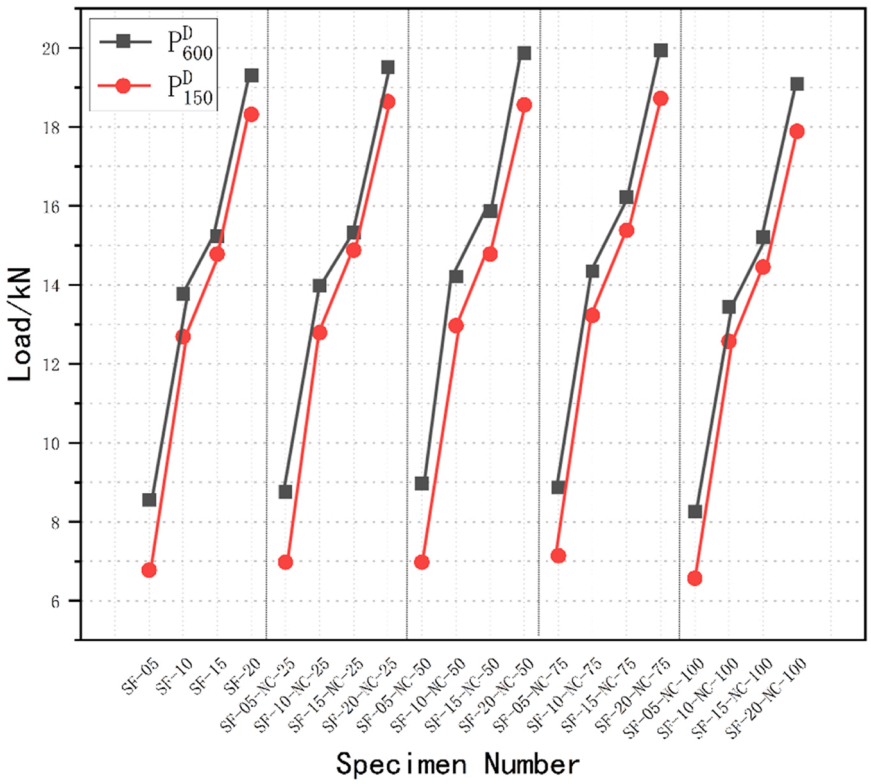

Fig. 8. Residual load P^D_{600} and P^D_{150} of the smart concrete mixes.

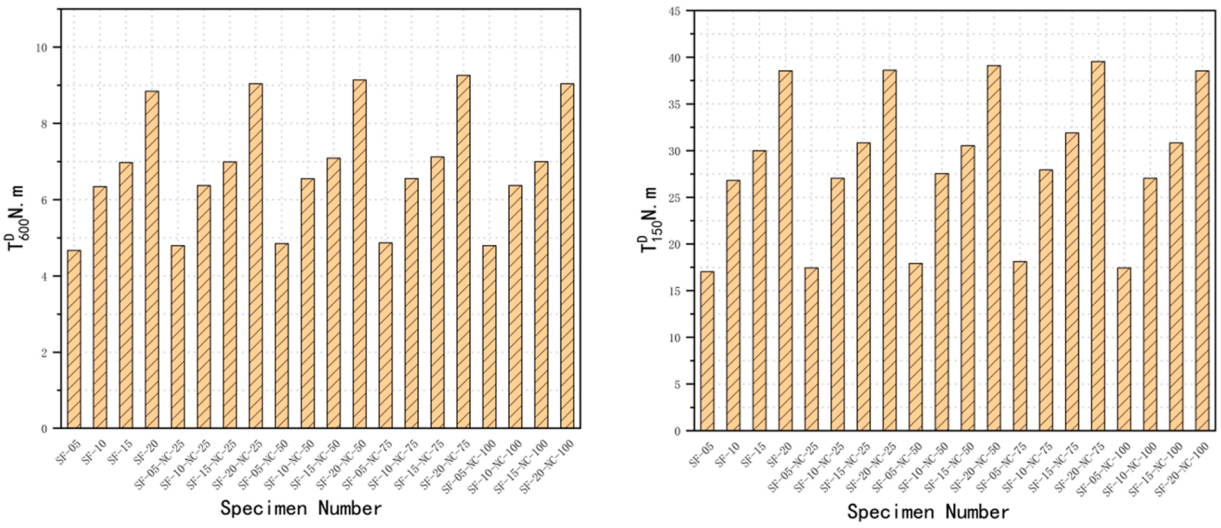

Fig. 9. Energy absorption values T^D_{600} and T^D_{150} of the smart concrete mixes.

corresponding to the strength of the smart concrete beam specimen with steel fiber and carbon black nanoparticles. As the concrete beam specimens for PC and those with only carbon black nanoparticles addition (i.e. without SF) showed brittle failure no toughness index data could be obtained.

The residual loads at the flex span ratio of 1/600 and 1/150 are analyzed as examples below. Fig. 8 shows the residual loads of smart concrete mixes. As expected the residual loads showed significant increase with the increase of the steel fibre content, while the NCB dosage had only minor effect. The SF-20-NC-75 mix showed the highest residual load and of the SF-05-NC-100 mix the lowest. The increase of residual loads, thus the increased residual bearing capacity of the smart concrete beam after cracking and enhanced safety of the component, is most likely due to the steel fiber bridging the cracks and reducing/restraining the crack propagation and improve the post-cracking bending toughness owing to gradual bond slip and fibre pullout.

3.3.2.2. Energy absorption value T^D_{600} *and* T^D_{150}. Fig. 9 shows the energy absorption values of the smart concrete mixes. It is not a surprise to see

Table 8
Equivalent flexural strength ratio of smart concrete.

Specimen number	$R^{D}_{T,150}$	Specimen number	$R^{D}_{T,150}$
SF-05	57.23	SF-15-NC-50	86.66
SF-10	83.91	SF-20-NC-50	101.36
SF-15	84.83	SF-05-NC-75	62.18
SF-20	100.45	SF-10-NC-75	86.57
SF-05-NC-25	59.12	SF-15-NC-75	89.8
SF-10-NC-25	83.51	SF-20-NC-75	102.01
SF-15-NC-25	86.78	SF-05-NC-100	59.85
SF-20-NC-25	100.74	SF-10-NC-100	85.08
SF-05-NC-50	60.15	SF-15-NC-100	87.82
SF-10-NC-50	85.34	SF-20-NC-100	100.24

that the energy absorption values of the smart concrete increases with the increase in steel fiber content, but show only minor changes to the varying carbon black nanoparticle dosage. The results also confirm the best performing mix being SF20-NC75, which showed the highest $T^{D}_{600}$and T^{D}_{150}values of 9.262 N·m and 39.538 N·m, respectively.

3.3.2.3. Equivalent bending strength ratio $R^{D}_{T,150}$. Table 8 shows the equivalent flexural strength ratio of the smart concrete mixes and Fig. 10 shows the bar chart of the results.

The results in Table 8 showed that the equivalent bending strength ratio of the smart concrete mixes increased with the increase of the steel fiber content, which reflects the improvement of the toughness of the concrete beam by steel fibers. Particularly, the SF20-NC75 mix achieved the highest equivalent bending strength ratio of 102.01. Also, all the smart concrete mixes with 2 % SF content (i.e. SF20, SF20-NC25, SF20-NC50, SF20-NC75, and SF20-NC100) achieved equivalent bending strength ratio greater than 100 %. Using the equivalent flexural strength ratio, we can judge whether the smart concrete has deflection/strain hardening. When the equivalent flexural strength ratio is greater than 100 %, the smart concrete is likely to show deflection/strain hardening.

To sum up: the bending toughness,the energy absorption and the residual load all increased with increase of steel fiber content for the smart concrete studied. The addition of carbon black nanoparticles only had a minor toughening effect on smart concrete, with an optimal NCB dosage at 0.75 %.

4. Electrical conductivity test of smart concrete

Self-monitoring smart concrete is a kind of concrete with multiple functions. Assessment of extent of damage and crack width in concrete structure is achieved by monitoring its resistance change rate through its overall conductivity. A good monitoring performance of smart concrete is inseparable from the addition of conductive materials. Different types of conductive materials and their addition dosages have different influences on the conductive properties of concrete, and their effectiveness in smart concrete is also different. Therefore, it is necessary to study various types and dosages of conductive materials incorporated into the concrete matrix in order to establish the suitable types of conductive materials and their optimal dosages so that the resulting concrete not only satisfying the basic requirement in mechanical properties, but also laying a foundation for achieving self-monitoring performance of smart concrete in the future.

4.1. Conductive mechanism of smart concrete

Song [24] and Forde M [25] et al. showed that concrete is not an insulator in a strict sense. Layssi H [26] and Sengul O [27] et al. pointed out that the pore solution in the matrix of ordinary concrete provides a conductive path, but the resistance of plain concrete is very high.

When a certain amount of conductive materials such as steel fiber and nano carbon black are added, steel fiber and nano carbon black can cooperate to exert long-range and short-range conduction respectively, and form a conductive network through the conductive filler and tunnel effect [28–30], so that concrete has good conductive property. In addition, when the smart concrete is subjected to load, initiation and growth of internal cracks, spacing or separation of steel fibres and their

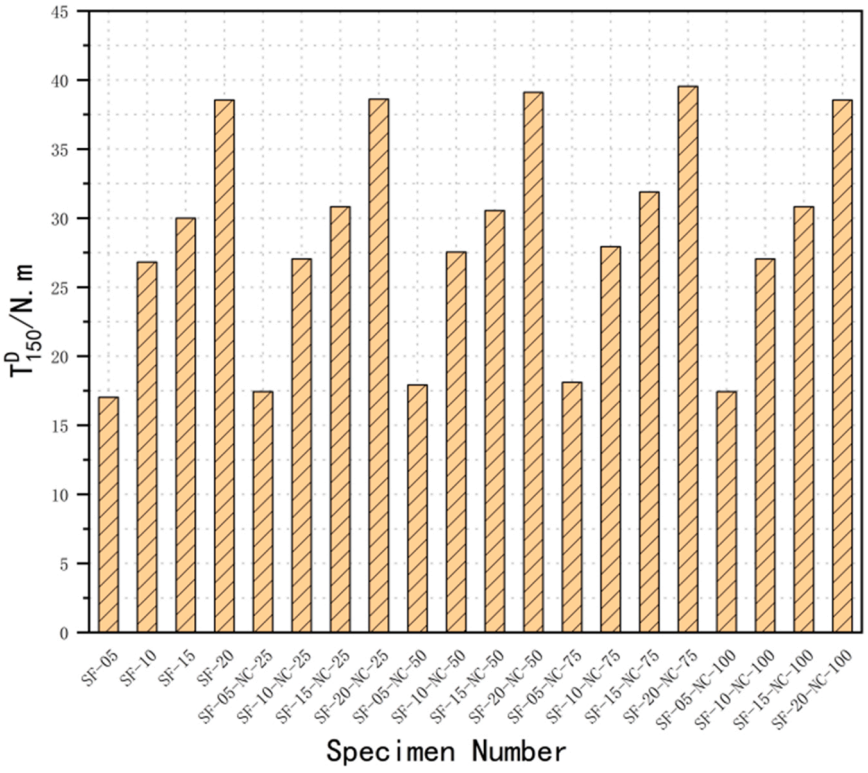

Fig. 10. smart concrete equivalent bending strength ratio $R^{D}_{T,150}$.

(a)Resistance measurement connection physical diagram

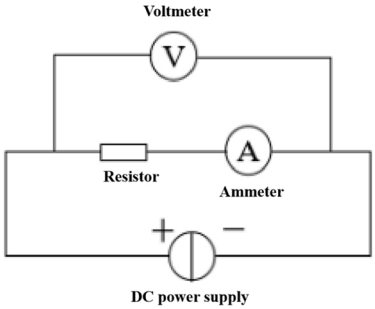

(b)Voltammetry to measure resistance

Fig. 11. smart concrete resistance measurement and electrode arrangement.

Table 9
volume resistivity of the concrete mixes.

Specimen number	Resistivity (Ω·m)	Specimen number	Resistivity (Ω·m)	Specimen number	Resistivity (Ω·m)
PC	160108	SF-05-NC-25	63466	SF-05-NC-75	15873
SF-05	73443	SF-10-NC-25	5367	SF-10-NC-75	2393
SF-10	7237	SF-15-NC-25	3278	SF-15-NC-75	1843
SF-15	3660	SF-20-NC-25	3353	SF-20-NC-75	2061
SF-20	3545	SF-05-NC-50	51254	SF-05-NC-100	26291
NC-25	88857	SF-10-NC-50	3622	SF-10-NC-100	4997
NC-50	55200	SF-15-NC-50	2177	SF-15-NC-100	2363
NC-75	24000	SF-20-NC-50	2394	SF-20-NC-100	2338
NC-100	64861	–	–	–	–

bond strength with the smart concrete matrix can all have an effect on the resistance of the smart concrete.

4.2. Smart concrete conductive performance testing

4.2.1. Test equipment and scheme

The test equipment include Shenzhen Xinyang double-sided conductive tape; Dc regulated power supply with a measuring range of 0–50 V, used to provide DC power supply, and display the measured voltage; and a Microammeter with a measuring range of 0–200μA, used to measure smart concrete flow current. The smart concrete test block used is the 100 mm × 100 mm× 100 mm specimen, and the specimen preparation process is described in Section 2.1.3.

The resistance test of all the concrete mixes shown in Table 4, including the control mix (i.e. PC) and smart concrete mixes with individual SF and NCB additions as well as with hybrid conductive materials was studied.

4.2.2. Smart concrete resistance measurement method

Voltammetry method was used to measure the resistance of smart concrete, that is, using an ammeter and voltmeter to measure the resistance value of smart concrete specimens. The most basic principle equation is the derivation of Ohm's law: R=U/I. According to the position of the ammeter (relative voltmeter), voltammetry can be divided into two kinds of resistance measurement, internal and external methods. Because the resistance value of smart concrete is far greater than that of the voltmeter, the external connection method will lead to the current through the voltmeter being far greater than that through the smart concrete, resulting in serious experimental error. The resistance value of the ammeter with the internal connection method, however, is much smaller than that of the smart concrete, and its voltage is very small, which makes the measured data more accurate. Therefore, the internal connection method was adopted in this study for measuring the resistance of the smart concrete,as shown in Fig. 11.

4.2.3. Smart concrete resistivity calculation method

According to the basic electrical formula, $J = E/\rho$, when the electric field intensity E is constant, the smaller the volume resistivity ρ of smart concrete, the greater the current density J is. The resistivity of a material can be determined by measuring the voltage and current density. When the concrete structure is damaged and cracked, the resistivity ρ of smart concrete becomes larger, and leading to smaller current density J. For achieving better self-monitoring performance of smart concrete, it is beneficial to have a small initial value of resistance (i.e. prior to damage/cracking) and a large range of change in resistivity during testing.

4.3. Test results and analysis of electrical conductivity of smart concrete

4.3.1. Electrical conductivity test results of smart concrete

To minimise the influence of other factors on the test results, three replicate cube specimens of each concrete mixes were tested at the same curing age. For each specimen tests were carried out using all three opposite sides. To avoid the interference of impurities on the surface of the specimen to the electrical signal, it was necessary to wipe the test surface with alcohol before applying the conductive tape. The volume resistivity values of all the concrete mixes obtained via measurement, analysis and calculation are shown in Table 9.

4.3.2. Analysis of resistivity results of concrete mixes with individual conductive materials

It could be noted that when the content of conductive material was small, the addition of conductive material would decrease the resistivity slightly. However, when the content of conductive material reached a certain level, the resistivity of the smart concrete showed a sharp drop. Further increase of conductive materials content could reach a critical content value, called the percolation threshold, beyond which no significant change in resistivity was observed Fig. 12 (a) and (b) plot the logarithmical values of the resistivity results against the SF and NCB contents, respectively.

As can be seen from Fig. 12 (a) and Table 9, the electrical resistivity decreased with the increase of steel fibre content. When the content of steel fiber reached 1.5 %, the resistivity decreased by 99.43 %, and the concrete material showed good electrical conductivity. It is apparent also that 1.5 % SF content is the percolation threshold of the electrical conductivity for such concrete mixes. It is believed that due to the relatively long fibre length the steel fiber addition has a good long-range conductive effect. The fibres can conduct across voids or cracks, which has an impact on the resistivity of smart concrete.

According to Fig. 12 (b) and Table 9, the resistivity also decreased when the content of carbon black nanoparticles increased initially.

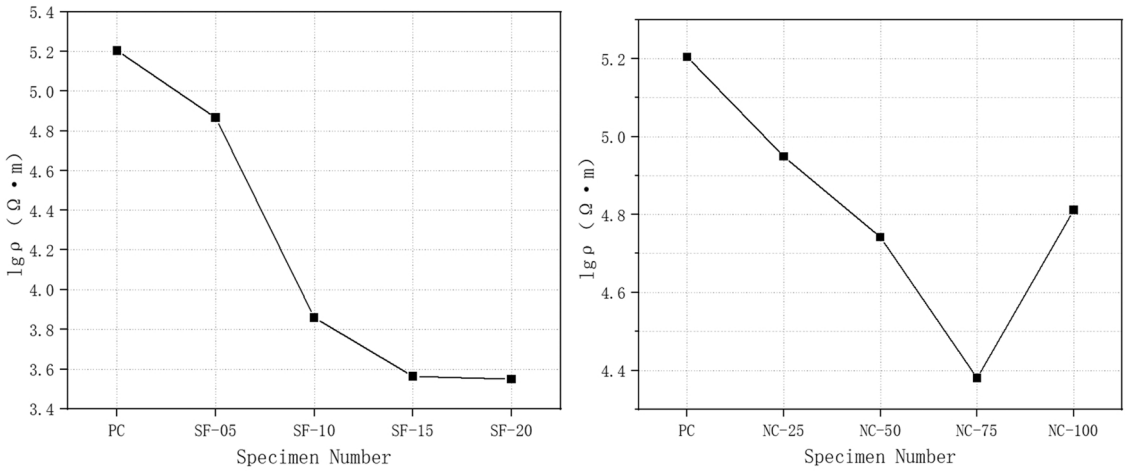

(a) Addition of steel fiber (b)Addition of nano carbon black

Fig. 12. Effect of addition of individual conductive materials on volume resistivity of concrete.

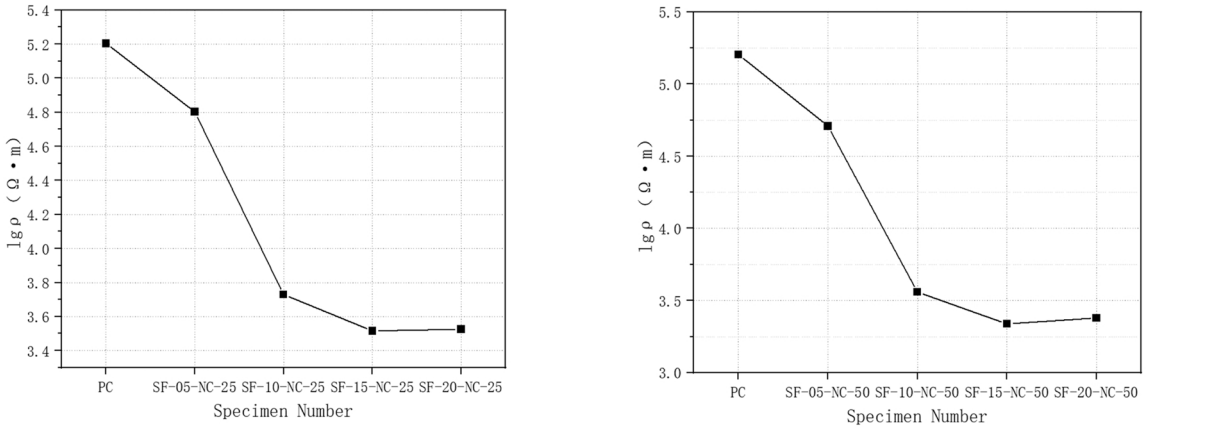

(a) Mixed steel fiber and nano carbon black(0.25%) (b) Mixed steel fiber and nano carbon black(0.5%)

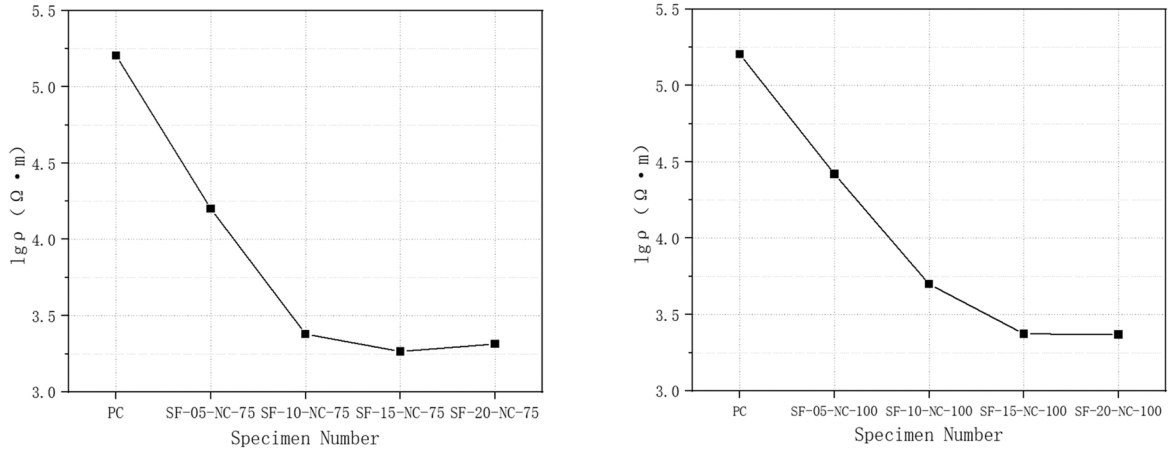

(c) Mixed steel fiber and nano carbon black(0.75%) (d) Mixed steel fiber and nano carbon black(1%)

Fig. 13. Volume resistivity results of smart concrete with hybrid conductive materials.

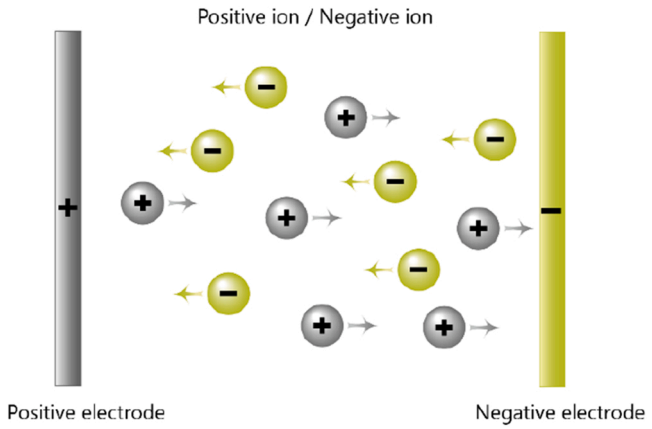

Fig. 14. Sketch of polarization in concrete [32].

When the content of carbon black nanoparticles reached 0.75 %, the resistivity decreased by 96.25 % compared to that of ordinary concrete (PC). Further increase in carbon black nanoparticle content (i.e. to 1.0 %), the resistivity showed an increase instead of decrease. Therefore, the 0.75 % content of carbon black nanoparticles is the percolation threshold. It is possible that high nano-carbon black content might have led to more air trapped in concrete, resulting in an increase of internal porosity of the concrete and thus reduced conductivity of the concrete mix.

4.3.3. Analysis of resistivity of smart concrete with hybrid conductive materials

Similar to Fig. 13 plots the logarithmical values of the resistivity results of all the smart concrete mixes with hybrid conductive materials.

As shown in Fig. 13 and Table 9, at the constant content of nano carbon black the resistivity of the smart concrete mixes increased with the increase of steel fiber content. Compared to the resistivity of concrete with individual conductive materials, the resistivity of the smart concrete mixes with hybrid conductive materials showed further significantdecreases., This demonstrates the beneficial effect of using the hybrid conductive materials and justify the use of the steel fiber together with the nano-carbon black for such smart concrete mixes.It is likely that in such smart concrete mixes with hybrid conductive materials the long-range conductive of steel fiber and the short-range conductive of nano-carbon black particles worked well together.

The results in Table 9 also show that the electrical conductivity was at its highest (i.e. resistivity at its lowest) when the carbon black content was 0.75 % and the steel fiber content was 1.5 %, regardless of using individual or hybrid conductive materials.

5. The crack self-monitoring test of smart concrete beams

5.1. The polarization effect of smart concrete

The polarization effect refers to the phenomenon that centers of the positive and negative charges of the monitored smart concrete specimens do not overlap at the initial stage of the test [31]. Within a period after the circuit is connected, under the action of an external electric field the positive and negative ions in the pore solution of the concrete matrix will move and aggregate towards the opposite electrodes, forming a gradual increasing counter electric potential phenomenon at the external electrodes [32]. Such polarization effectwill affect the monitoring results of the smart concrete resistance. The schematic diagram of polarization is shown in Fig. 14. To minimise the influence of the polarization effect in this test, it is necessary to run the electricity for half an hour before the test loading, and then conduct the test when the measured current is stable [33]. Dc constant voltage power supply or AC constant voltage power supply can be used for the measurement of resistance. In this test, a DC constant voltage power supply was used for monitoring the tension zone of the smart concrete test beam. Dc power supply will also produce polarization phenomenon, so it is necessary to consider the influence of polarization phenomenon on resistance monitoring.

5.2. Test overview

To avoid the influence of the contact resistance between the concrete matrix and the electrode, it is necessary to dry and clean the concrete beam specimen to remove residual oil and other impurities from the specimen surface before starting the test. It was noticed that the impurities remained on the surface of the smart concrete could seriously interfere with the input and output of the current and the accuracy and stability of the electrical signal measurement. As a result, the contact resistance would increase and the final test results affected.

5.2.1. Calculation of surface resistance change rate in tensile zone of smart concrete beam

Because the smart concrete beam specimen is an irregular conductive matrix when cracking under load, there will be errors in the results when taking the resistance or resistivity as the standard. To facilitate the

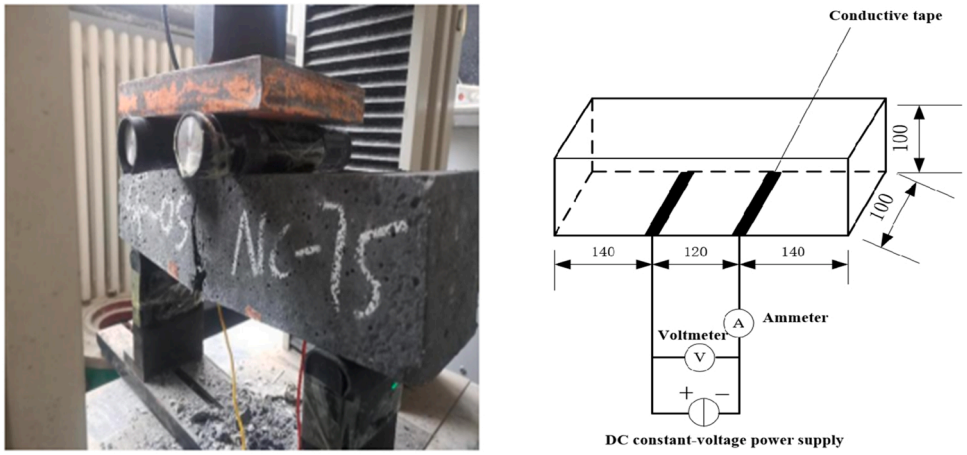

(a) 4-point bending test (b) Circuit diagram

Fig. 15. Test setup and circuit diagram of smart concrete electrical signal acquisition device.

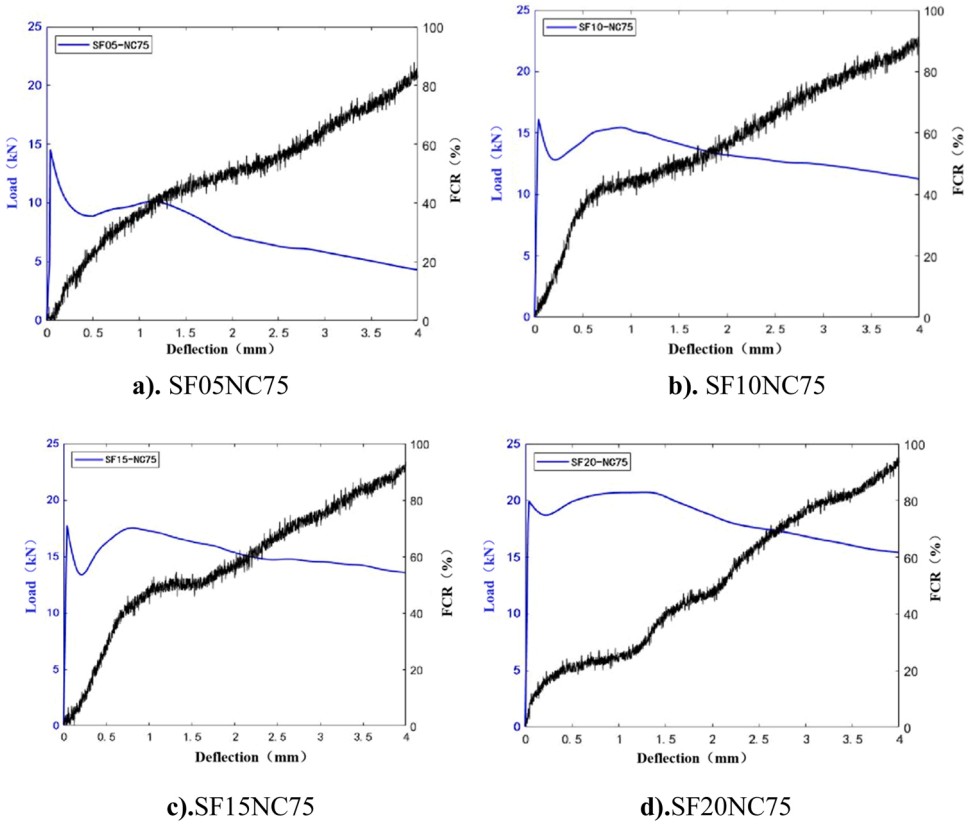

Fig. 16. load and resistance change rate vs mid-span deflection.

analysis, the resistance changes are normalized, so that resistance change rate (Fractional change in resistance, FCR) or resistance change percentage is used as a measureof resistance change [34–36]. At constant voltage, surface resistance change rate in tensile zone of smart concrete beam is calculated using the following formula:

$$FCR = \left(\frac{I_0}{I_A} - 1\right) \times 100\% \quad (4)$$

In the formula, FCR is resistance change rate (%). I_0 is initial current value (A). I_A is real-time current value (A).

According to Eq. (4), when the voltage is a constant value, the test only needs to measure the initial current and monitor the current in real-time to calculate the resistance change rate.

Based on the results obtained for mechanical properties and electrical conductivity as presented and discussed above, smart concrete with 0.75 % NCB achieved good overall electrical conductivity and mechanical properties. Therefore, it was decided to only use smart concrete mixes with 0.75 % NCB dosage and various steel fiber contents for the smart concrete crack self-monitoring test.

5.2.2. *Electrode arrangement*

In the crack self-monitoring test of the smart concrete beam specimen, the external two-electrode method was used to measure and collect electrical signals. The electrodes were placed in the tension zone of the smart concrete beam specimen to monitor the surface resistance change rate of the area under load and the resistance change rate of the cracking. Before the test, the specimen was polished, and alcohol was used to wipe the external electrode attachment [37]. The external electrode method was adopted, and the electrode material was 20 mm wide double-sided conductive tape.

Combined with the bending moment diagram and shear diagram, the electrodes are arranged in the section where cracks are not easy to occur. The distance between the two electrodes is 120 mm. The test setup and the electrode arrangement is shown in Fig. 15(b).

5.2.3. *Loading method*

The crack self-monitoring test of the smart concrete beam specimen was carried out simultaneously with the bending toughness test, that is, during the four-point loading process, the surface resistance change rate of the concrete under tension area and the resistance change rate at the time of cracking were monitored simultaneously. Test by 100 kN microcomputer control electro-hydraulic servo hydraulic pressure testing machine control loading set the loading rate of 0.01 kN/s and limit failure criteria, through the sensor automatic collection of specimen span deflection (because the specimen span is very small ignore the bearing deflection), from 0 to apply the load to reach the ultimate load, minimal deflection does not test the crack, After reaching the ultimate load, the deflection increases significantly. Test the crack once with the vernier caliper for each load change of 0.5 kN. The ES21B current acquisition module was used to collect the data on current changes, and the sampling frequency was set as 50 Hz. The DC voltage value remained unchanged and the current was taken as the variable to further calculate the resistance change rate. Since the resistance of the concrete beam specimen under tension was relatively large, the external connection method was used for real-time monitoring. Data acquisition is carried out when the electrical signal is stable. The test process and circuit diagram of electrical signal acquisition are shown in Fig. 15.

5.3. *Analysis of resistance change rate in tensile region under load*

The load-deflection curve was directly drawn by the computer in the test, the resistance was calculated according to the collected current, and the volume resistivity was calculated. The load and resistance change rate (i.e. FCR) vs mid-span deflection curves for the smart concrete beam with hybrid conductive materials are shown in Fig. 16.

As shown in Fig. 16, the resistance of the smart concrete beam

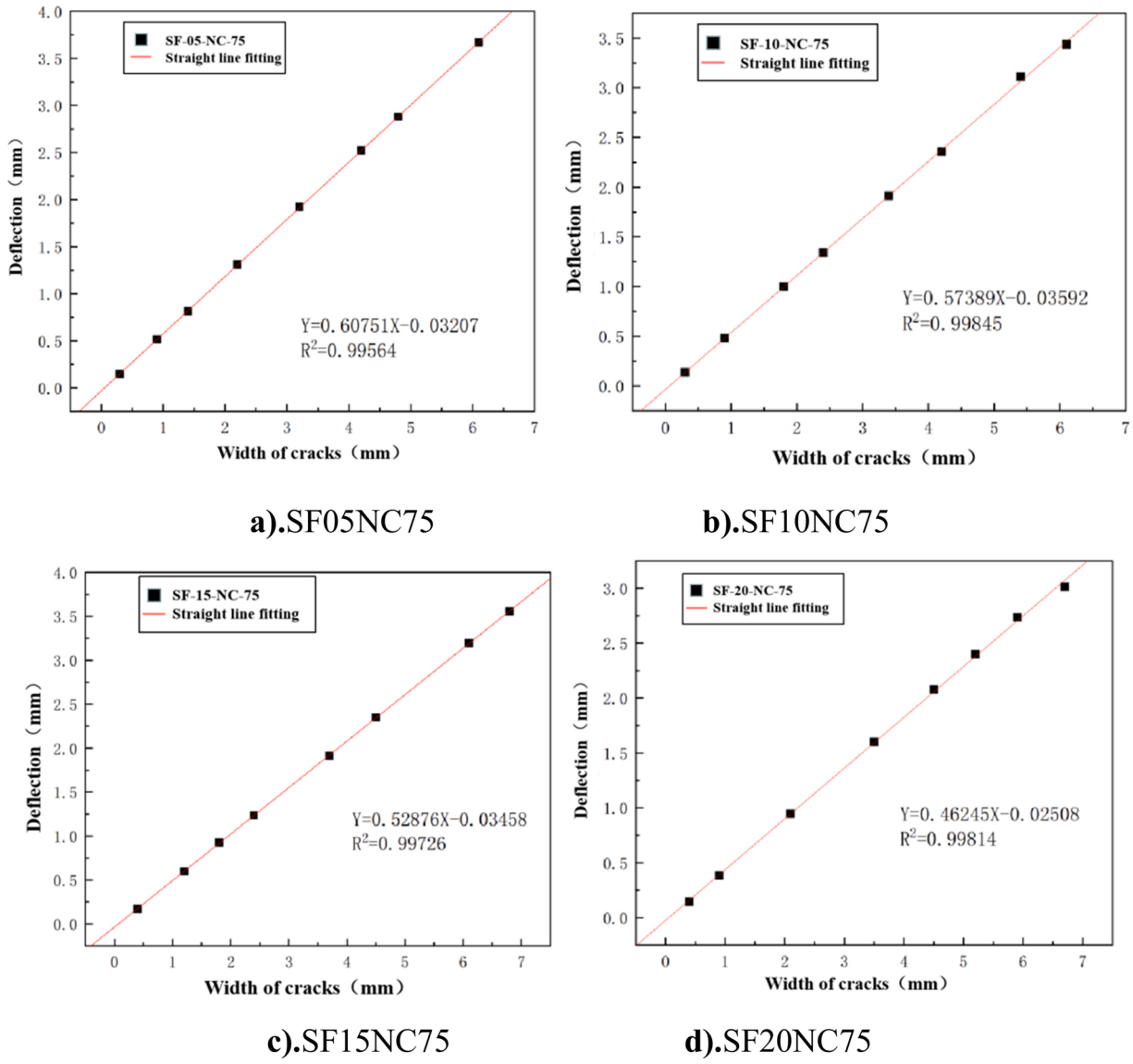

Fig. 17. Fitting curve of crack width and deflection.

Table 10
Linear fitting parameters.

Specimen number	Slope	Intercept	R^2
SF05NC75	0.60751	-0.03207	0.99564
SF10NC75	0.57389	-0.03592	0.99845
SF15NC75	0.52876	-0.03458	0.99726
SF20NC75	0.46245	-0.02508	0.99814

specimens did not change significantly before cracking, but at the moment of cracking, the change rate of resistance increased instantly, and the cracking load of the SF-20-NC-75 group was the largest. After cracking, the bearing capacity gradually decreased and the resistance change rate became higher and higher. The surface resistance change rate of the tensile area of the specimen gradually increased with the increase of mid-span deflection. The main reason was that with the hybrid conductive materials used, the specimens benefited from the long-range conductivity effect of steel fibers and the short-range conductivity effect of nanoparticles [38–40]. After loading, the steel fiber inside the concrete would debond and slip, which increases the contact electric resistance. With further increase in mid-span deflection, the steel fiber would be pulled out and cracks widened.The resistance increased with increase of mid-span deflection and cracks width.

5.4. Relationship between mid-span deflection and crack width of beam specimen

To study the relationship between crack width and resistance change rate, the deflection and crack width of the smart concrete beam specimen after cracking were analyzed correspondingly, and the measured data fitted and analyzed using software package Origin, as shown in Fig. 17 and Table 10.

It can be seen from Table 10 that the R^2 of the fitting curves are all greater than 0.995, indicating that the linear fitting results are excellent and the test results can be reliably predicted using the linear regression model. At the same time, it can be proved that there is a certain proportional relationship between the crack width and the mid-span deflection of the smart concrete beam specimen after cracking. The crack width of the smart concrete with different contents of steel fiber can be further calculated by using the mid-span deflection through the fitting formula, to determine the relationship between the crack width and the resistance change rate.

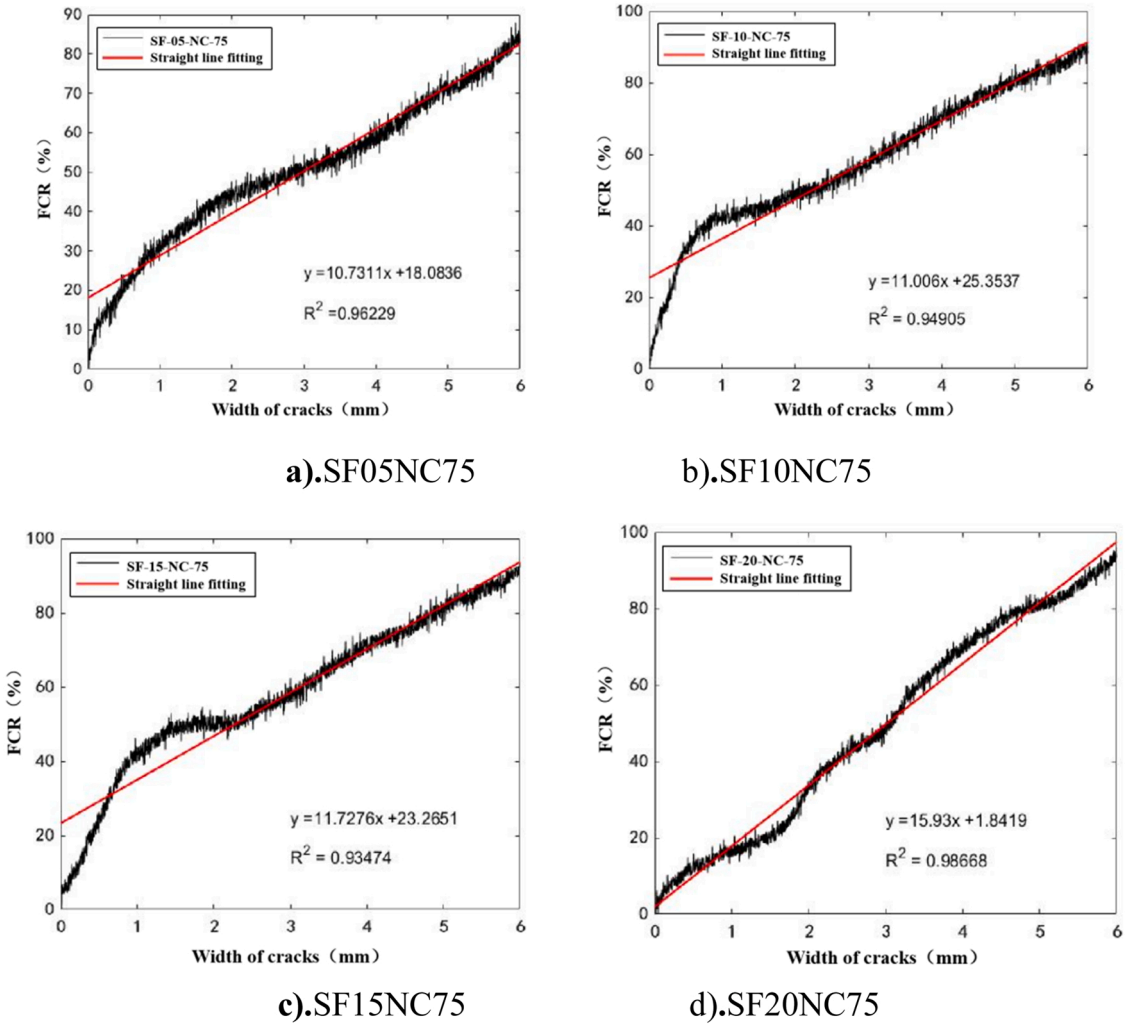

Fig. 18. crack width and resistance change rate fitting curve.

Table 11
Linear fitting parameters.

Specimen number	Slope	Intercept	R2
SF05NC75	10.7311	18.0836	0.96229
SF10NC75	11.006	25.3537	0.96229
SF15NC75	11.7276	23.2651	0.99726
SF20NC75	15.93	1.8419	0.98668

5.5. The relationship between crack width and resistance rate of change

To study the relationship between crack width and resistance change rate of the smart concrete beam specimen after cracking, the four linear regression models established in Section 5.4 were used to plot the FCR vs crack width curves for the smart concrete beams, as shown in Fig. 18 and Table 11.

It can be seen from Table 11 that the determination coefficients of the fitting curves are all greater than 0.96, indicating that the conclusion of the linear fitting is reasonable, and the relationship between crack width and resistivity can be predicted based on the linear regression model. In addition, it can be seen that in the bending loading process of the smart concrete beam specimen, the crack width of the pure bending section is positively correlated with the resistance change rate, and the slope of the fitting curve gradually increases with the increase of the steel fiber content, while there is no clear relationship between the fiber content and the intercept.

The test results show that: There is a clear correlation between the crack width and the resistance change rate. With the increase of the steel fiber content, the change amplitude of the resistance at a given crack width become greater, indicating a better monitoring effectiveness of the smart concrete. This confirms that reasonably good self-monitoring performance could be achieved using the smart concrete mixes with the hybrid conducive materials, and the monitoring effectiveness of smart concrete could be improved with the increase of the steel fiber content.

6. Conclusions

As a kind of multi-functional concrete, smart concrete not only has good working performance and mechanical properties, but also can monitor the damage of concrete, estimate the size of cracks, and thus achieve timely feedback on the engineering safety state. Based on the results obtained in this in-depth experimental study of various smart concrete mixes through the addition of steel fibre and nano carbon black conductive materials, the following conclusions are drawn:

(1) By conducting experiments on smart concrete materials, the effects of milled steel fibers, and carbon black nanoparticles on the conductive properties of smart concrete are compared. The percolation threshold for the content of carbon black nanoparticles was found to be 0.75 % (NC-75). For the content of steel fibre, it was 1.5 % (SF-15). The percolation threshold was reached

when 0.75 % nanocarbon black and 1.5 % milled steel fiber were used together (SF-15-NC-75).

(2) Through the smart concrete cube compressive strength test, the influence of different mixtures of smart concrete materials on compressive strength was studied. It was found that the effect of steel fibre addition could significantly increase the compressive strength of the smart concrete, while the addition of carbon black nanoparticles had only very minor influence on the compressive strength.

(3) Through the bending toughness test of the smart concrete beam specimen, the influence of different mixtures of conductive materials on the bending toughness of the smart concrete beam was compared. The results clearly showed that: the steel fiber played a dominant role, with the increase of the milling steel fiber content leading to significant enhancement in flexural performance and much increased bending toughness. In comparison, the addition of carbon black nanoparticles had only very minor impact on the toughness.

(4) Through the test for self-monitoring of cracks of the smart concrete beam specimen, the relationship between the crack width and the resistance change rate of the selected smart concrete beam specimen using hybrid conductive materials were studied. The results show that before cracking, the resistance in the tensile zone did not change significantly. After the cracking, the crack width was found positively correlated with the resistance change rate. With the expansion of the crack width, the resistance in the tensile zone gradually increases.

(5) Smart concrete materials can be applied in the tension zone or protective layer of beam members, so that the concrete beam has the function of self-monitoring, while saving materials, but also can inhibit the expansion of cracks, which provides a new method and idea for the application of smart concrete materials in major engineering facilities to realize the self-monitoring of cracks.

CRediT authorship contribution statement

Jiuyang Li: Financial support, Conceptualization , Formal analysis , Writing - review & editing. **Li Chen:** Original Draft, Specimen Production , Formal analysis. **Guangchao Hu:** Specimen Production , Formal analysis. **Jinpeng Guo:** Specimen Production , Self monitoring test. **Zhenwei Wang:** Specimen Production , Self monitoring test. **Wenbo Lu:** Specimen Production , Project administration , Methodology. **Jingwei Luo:** Methodology. **Xinmei Fan:** Methodology. **Yuepeng Zhu:** Methodology. **Xiaoyu Wang:** Writing - review & editing. **Wenzhong Zhu:** Writing - review & editing.

Declaration of Competing Interest

The authors declare that they have no known competing financial interests or personal relationships that could have appeared to influence the work reported in this paper.

Data availability

The data that has been used is confidential.

Acknowledgements

This project is financially supported by Science and Technology Development Plan of Jilin Province (20210203178SF) and (20200602002ZP).

References

[1] H. Zhang, J. Li, F. Kang, et al., Monitoring and evaluation of the repair quality of concrete cracks using piezoelectric smart aggregates, Constr. Build. Mater. 317 (2022), 125775.
[2] M. El Mountassir, S. Yaacoubi, Dataset for structural health monitoring of pipelines using ultrasonic guided waves, Data Brief. 45 (2022), 108756.
[3] P.F. Giordano, S. Quqa, M.P. Limongelli, The value of monitoring a structural health monitoring system, Struct. Saf. 100 (2023), 102280.
[4] J. Etxaniz, G. Aranguren, J.M. Gil-García, et al., Ultrasound-based structural health monitoring methodology employing active and passive techniques, Eng. Fail. Anal. (2023), 107077.
[5] Z. Zhou, B. Zhang, K. Xia, et al., Smart film for crack monitoring of concrete bridges, Struct. Health Monit. 10 (3) (2011) 275–289.
[6] J.K. Zhang, W. Yan, D.M. Cui, Concrete condition assessment using impact-echo method and extreme learning machines, Sensors 16 (2016) 447.
[7] E. Hwang, G. Kim, G. Choe, M. Yoon, N. Gucunski, J. Nam, Evaluation of concrete degradation depending on heating conditions by ultrasonic pulse velocity, Constr. Build. Mater. 171 (2018) 511–520.
[8] M.K. ElBatanouny, P.H. Ziehl, A. Larosche, J. Mangual, F. Matta, A. Nanni, Acoustic emission monitoring for assessment of prestressed concrete beams, Constr. Build. Mater. 58 (2014) 46–53.
[9] D. Eisenmann, F.J. Margetan, L. Koester, D. Clayton, Inspection of a large concrete block containing embedded defects using ground penetrating radar, AIP Conf. Proc. (2016) 1706.
[10] Yang Jie, Zhang Kai, Cheng Lin, Zhaohan Wang, Yaming Li, A fiber optic sensor for crack monitoring of concrete structures, Piezoelectricity Acoustooptics 41 (04) (2019) 481–484.
[11] Zhang Hong-Jian, Kong Yan, Zhao Qi-Lin, Fan Yu-Xin, Li Jin-cheng, Review on the development of concrete crack monitoring and detection technology, Mod. Transp. Technol. 16 (04) (2019) 42–48.
[12] J. Yan, A. Downey, A. Cancelli, et al., Concrete crack detection and monitoring using a capacitive dense sensor array, Sensors 19 (8) (2019) 1843.
[13] Heng Zhen. Self-monitoring Performance of intelligent Concrete Cracking and Influence of Temperature and Humidity, Dalian University of Technology, 2017 (in Chinese).
[14] Li Fei, Peng Ziqiang, Shi Xian, Wu Longbiao, Research progress of concrete crack detection and monitoring technology, Guangdong Civ. Constr. 29 (05) (2022) 96–99+115.
[15] D. Luo, Y. Yue, P. Li, et al., Concrete beam crack detection using tapered polymer optical fiber sensors, Measurement 88 (2016) 96–103.
[16] Lin Wei-hao, Sun Siming, Hu Jie, Zhao Fang, S.H.A.O. Li-yang, Research and application of sensing technology based on fiber ring laser, Semicond. Optoelectron. 43 (04) (2022) 728–737.
[17] E. García-Macías, A. D'Alessandro, R. Castro-Triguero, et al., Micromechanics modeling of the uniaxial strain-sensing property of carbon nanotube cement-matrix composites for SHM applications, Compos. Struct. 163 (2017) 195–215.
[18] E. García-Macías, R. Castro-Triguero, A. Sáez, et al., 3D mixed micromechanics-FEM modeling of piezoresistive carbon nanotube smart concrete, Comput. Methods Appl. Mech. Eng. 340 (2018) 396–423.
[19] Liugen Jin, Ding Yining, Heng Zhen, Influence of different electrical conductivity on sensitivity and noise level of intelligent Self-monitoring of concrete crack, J. Compos. Mater. 20 (37) (2023) 2610–2618 (in Chinese).
[20] A.O. Monteiro, P.B. Cachim, P.M.F.J. Costa, Self-sensing piezoresistive cement composite loaded with carbon black particles, Cem. Concr. Compos. 81 (2017) 59–65.
[21] S. Wen, D.D.L. Chung, Partial replacement of carbon fiber by carbon black in multifunctional cement–matrix composites, Carbon 45 (3) (2007) 505–513.
[22] GB/T 50081-2019, Test method standard for physical and mechanical properties of concrete. Beijing: China Architecture and Building Press, 2019.(in Chinese)
[23] ASTM C1609M-12. Flexural Performance of Fiber-Reinforced Concrete (Using Beam With Third-Point Loading). West Conshohocken, PA: ASTM International, 2012.
[24] G. Song, Equivalent circuit model for ac electrochemical impedance spectroscopy of concrete, Cem. Concr. Res. 30 (11) (2000) 1723–1730.
[25] M. Forde, J. McCarter, H. Whittington, The conduction of electricity through concrete, Mag. Concr. Res. 33 (114) (1981) 48–60.
[26] H. Layssi, P. Ghods, A. Alizadeh, et al., Electrical resistivity of concrete, Concr. Int. 37 (5) (2015) 41–46.
[27] O. Sengul, 0 Gjørv, Effect of embedded steel on electrical resistivity measurements on concrete structures, Acids Mater. J. 106 (1) (2009) 11–18.
[28] B. Han, L. Zhang, S. Sun, et al., Electrostatic self-assembled carbon nanotube/nano carbon black composite fillers reinforced cement-based materials with multifunctionality, Compos. Part A: Appl. Sci. Manuf. 79 (2015) 103–115.
[29] B. Han, S. Sun, S. Ding, et al., Review of nanocarbon-engineered multifunctional cementitious composites, Compos. Part A: Appl. Sci. Manuf. 70 (2015) 69–81.
[30] B. Han, Y. Wang, S. Ding, et al., Self-sensing cementitious composites incorporated with botryoid hybrid nano-carbon materials for smart infrastructures, J. Intell. Mater. Syst. Struct. 28 (6) (2017) 699–727.
[31] S. Wen, D.D.L. Chung, Electric polarization in carbon fiber-reinforced cement, Cem. Concr. Res. 31 (1) (2001) 141–147.
[32] Xie Haowei, Effect of Steel Fiber on Crack Self-monitoring Performance of Intelligent Concrete. Dalian University of Technology.(in Chinese).
[33] T.-C. Hou, J.P. Lynch, Conductivity-based strain monitoring and damage characterization of fiber reinforced cementitious structural components. Smart Structures and Materials 2005: Sensors and Smart Structures Technologies for

Civil, Mechanical, and Aerospace Systems 5765, International Society for Optics and Photonics, 2005, pp. 419–430.
[34] W. Wang, H. Dai, S. Wu, Mechanical behavior and electrical property of CFRC-strengthened RC beams under fatigue and monotonic loading, Mater. Sci. Eng.: A 479 (1–2) (2008) 191–196.
[35] C. Jiang, Z. Li, X. Song, et al., Mechanism of functional responses to loading of carbon fiber reinforced cement-based composites, J. Wuhan. Univ. Technol. -Mater. Sci. Ed. 23 (4) (2008) 571–573.
[36] J. Xu, W. Zhong, W. Yao, Modeling of conductivity in carbon fiber-reinforced cement-based composite, J. Mater. Sci. 45 (13) (2010) 3538–3546.
[37] Wang Ling, Luo Ke, Li Ziqiang, et al., Experimental device and application of small electrode for resistivity measurement of mineral and solid insulating materials, Sci. China.: Sci. Technol. 7 (2011) 890–895.
[38] F.J.B. Calleja, R.K. Bayer, T.A. Ezquerra, Electrical conductivity of polyethylene-carbon-fibre composites mixed with carbon black, J. Mater. Sci. 23 (4) (1988) 1411–1415.
[39] S. Wu, L. Mo, Z. Shui, et al., Investigation of the conductivity of asphalt concrete containing conductive fillers, Carbon 43 (7) (2005) 1358–1363.
[40] X. Liu, S. Wu, N. Li, et al., Self-monitoring application of asphalt concrete containing graphite and carbon fibers, J. Wuhan. Univ. Technol. -Mater. Sci. Ed. 23 (2) (2008) 268–271.